Evaluation of NF membranes as treatment technology of acid mine drainage: metals and sulfate removal

J. Lopez*[a,b], M.Reig[a,b], O. Gibert[a,b,c], C.Valderrama[a,b] and J.L.Cortina[a,b,c]

[a] Chemical Engineering Department, UPC-BarcelonaTECH, C/ Eduard Maristany, 10-14 (Campus Diagonal-Besòs), 08930 Barcelona, Spain

[b] Barcelona Research Center for Multiscale Science and Engineering, C/ Eduard Maristany, 10-14 (Campus Diagonal-Besòs), 08930 Barcelona, Spain

[c] Water Technology Center Cetaqua, Carretera d'Esplugues 75, 08940 Cornellà de Llobregat, Spain

*Correspondence should be addressed to: Julio Lopez

Tel.: (34)93 4016997;

Email: julio.lopez.rodriguez@upc.edu

Abstract (max. 200 words)

Acid mine drainage (AMD) are acidic streams rich in dissolved ferrous and non-ferrous metal sulfates and minor amounts of non-metals. Nanofiltration (NF) has been postulated as a potential technology in the metallurgical and mining industry to recover strong acids as H_2SO_4 and concentrate metallic ions from acidic mine waters. The performance of semi-aromatic polyamide (NF270) and sulfonated polyethersulfone (HydraCoRe 70pHT) NF membranes were evaluated at different trans-membrane pressures. Different synthetic solutions were filtered under spiral wound configuration at two pHs (2.0 and 2.8): i) a solution of Na_2SO_4 and ii) a solution mimicking AMD from dams, containing Na_2SO_4 and Fe^{2+}, Zn^{2+} and Cu^{2+}. NF270 showed metal rejections higher than 90 %, while for HydraCoRe 70pHT they were in between 60 and 70%. Metal rejection values decreased when solution acidity was increased. Chemical composition of the membrane active

layer and the aqueous metal-sulfate speciation were found to have a large impact on membrane separation process. Solution-Electromigration-Diffusion-Film model was used to estimate the membrane permeances to ions from the measured ion rejections. Furthermore, a full scale unit vessel containing six spiral wound membrane modules was simulated. NF270 showed a higher capacity for concentrating metal and sulfate ions (100%) than Hydracore 70pHT (50%).

Keywords: Acid mine drainage; spiral wound; NF270; HydraCoRe 70pHT, metal recovery, SEDF model

1. Introduction

Acid mine drainage (AMD) are strong acidic streams rich in dissolved ferrous and non-ferrous metal sulfates, and non-metallic species (e.g., As, Se) [1] occurring in galleries, mine workings, open pits, waste rock piles, and mill tailings in both operating and abandoned poly-sulfide mining sites [2–4]. AMD generation is straightforward and its final composition is a function of the geochemistry of the mineral deposits, presence of oxygen, water availability, microorganisms and temperature [5]. Due to the environmental threats posed by AMD, research has been focused on the development of cost-effective and sustainable solutions for the AMD treatment [6]. However, despite AMD is identified as the main concern for mining and extraction industries, no single successful initiative has developed the required combination of scale, resources and affordability to deal with the problem.

The main effort to treat AMD has been allocated to the development of remediation techniques based on source control and migration control [7]. Source control techniques are directed towards controlling the formation of AMD at source and are based on avoiding the contact of oxygen and/or water with sulfide minerals [3,8,9]. Alternatively, sulfide oxidation can also be hindered by separating selectively sulfide minerals from the waste [8]. However, many attempts to prevent

AMD generation have proven to be unprofitable [10] with the risk of contaminating surrounding water bodies such as the underground aquifers. Different remediation options have been developed for the management of AMD once it has been generated and has eventually contaminated the surrounding water bodies. Among them are: i) its containment to prevent migration of contaminants (e.g., using geotechnical measures), ii) active treatments using an energy source (e.g., pump-and-treat systems, by which AMD-contaminated water is pumped, treated and, optionally, injected to the aquifer) and iii) passive treatments without any energy source (e.g., permeable reactive barriers, by which AMD-contaminated groundwater is treated in-situ by an appropriate reactive material placed under ground in the path of the polluted water flow) [11–15]. Few efforts have been made so far in treating AMD for the recovery of sulfuric acid and/or dissolved transition metals [5]. These studies have involved AMD treatment with traditional technologies (chemical precipitation, adsorption, coagulation–flocculation, flotation and electrochemical methods [16,17]), membrane technologies [18,19], ion-exchange membranes (IXM) [20], membrane distillation (MD) [21], forward osmosis (FO) [22] and reverse osmosis (RO) [23].

Some recent studies have proposed the treatment of AMD by nanofiltration (NF) [18,19,24–28]. NF has the additional advantage of selectively separating single-charged ions with a wide range of rejection values, which makes feasible to concentrate metallic ions and, at the same time, recover acids from AMD [29,30]. Research studies have highlighted that H_2SO_4 rejection by NF depends on its speciation. For instance, Visser et al. [25] treated sulfuric acid solutions with aromatic and semi-aromatic polyamide-based NF membranes and found that at neutral pH (pH>pKa=1.9), when sulfuric acid is presented mainly as SO_4^{2-}, the rejection percentage was higher than 99.9%, but at low pH (pH<pKa1.9), when the prevalent form of sulfuric acid is HSO_4^-, the rejection percentage was below 20%. Another factor that must be taken into account in the membrane performance is its iso-electric point (IEP), which is defined as the pH value at which

77 membrane exhibits zero charge [24]. It has been found that at pH lower than the IEP, the
78 membranes present a positively charged surface, thus leading to high metal rejection, attributed
79 to the positively charged membrane [18,19,23,24,31]. For example, Mullet et al. [24] filtered AMD
80 with two polyamide NF membranes (NF270 and TriSep TS80) working at recovery ratios of 70%
81 and observed that, at pH values lower than the IEP, cation rejection was maximized. Therefore,
82 as reported by these previous studies, sulfuric acid can be, under appropriate pH, recovered in
83 the permeate stream, while metal species are retained in the concentrated side.
84 Among the different models to describe the separation performance of a NF membrane, the
85 solution-diffusion model is widely applied [32–35]. Yaroschuck et al. [32] coupled the solution-
86 diffusion model to film model theory for single salts (Solution-Diffusion-Film model (SDFM)), and
87 latter extended to electrolyte mixtures (Solution-Electromigration-Diffusion-Film model (SEDFM))
88 [33–36]. SEDFM allows to obtain the membrane permeance to a given ion, which depends upon
89 both the membrane and ion properties.
90 This study evaluated the valorization of acidic mine waters, i.e. the recovery of sulfuric acid and
91 valuable metals (Fe, Zn and Cu) with two NF membranes under a spiral wound (SW)
92 configuration: a) semi-aromatic polyamide based composite membrane (NF270) and b) a
93 sulfonated polyethersulfone based composite membrane (HydraCoRe 70pHT). SEDFM was used
94 to determine the membrane permeances to ions. The main novelty of this work is the effort to
95 describe the transport mechanisms of ions in AMD through NF membranes taking into account
96 the different chemical properties of the membranes and the ions speciation. It must be stressed
97 that the HydraCoRe 70pHT is a novel membrane that has not been used to treat acidic waters
98 according to the literature review.
99

2. Materials and methods

2.1. Water composition

Two synthetic acid solutions of Na_2SO_4 (at pH 2.8 and 2.0) with and without metal ions (Fe^{2+}, Zn^{2+}, Cu^{2+}) were used in this study. Their composition is given in Table 1. The second type of water mimicked an AMD generated in a poly-sulfide mine in the South of Spain (Río Tinto). This mine is located in the South-Portuguese zone of the Iberian Peninsula, in the so-called Iberian Pyrite Bell, which is one of the main poly-sulfide deposits worldwide, mainly composed of pyrite (FeS_2), chalcopyrite ($CuFeS_2$), sphalerite (ZnS) and galena (PbS) [37]. The compositions of the synthetic waters were based on average values of the AMD stored in the pond of the mine along one year. Major components (Na^+, SO_4^{2-}, Fe^{2+}, Zn^{2+}, Cu^{2+}) were considered for the experimental design, while metals at concentrations below 20 mg/L (Ca, Mg and Al, among others) were not included. The two pH values were selected according to the limit values reported in the mining operation site

For the first type of water, a solution containing 0.1 M H_2SO_4 was prepared and NaOH 50% was carefully added until the desired pH value was obtained (2.8 and 2.0). For the second type of water mimicking an AMD, appropriate amounts of Fe, Cu, Zn from their respective sulfate salts were dissolved in the solution described above and pH was adjusted by the addition of H_2SO_4. Speciation diagrams obtained with Hydra/Medusa software [38] are shown in Annex I.

Table 1. Concentrations of the both types of water

pH	$[H^+]$ (mmol/L)	$[Na^+]$ (mmol/L)	$[SO_4^{2-}]$ (mmol/L)	$[Fe^{2+}]$ (mmol/L)	$[Zn^{2+}]$ (mmol/L)	$[Cu^{2+}]$ (mmol/L)
2.8	1.6	200	100	-	-	-
2.0	10	190	100	-	-	-
2.8	1.6	49	80	45	4	5
2.0	10	46	94	56	7	3

2.2. Membrane set-up and procedure

Two different membranes were tested under SW configuration: NF270 (from Dow Chemical) and HydraCoRe 70pHT (from Hydranautics). NF270 is a thin-film composite based on a semi-aromatic polyamide active layer, where carboxylic (R-COOH) and amine ($R-NH_2$) groups are present. NF270 has an IEP value of 3, and the membrane z-potential has a value of 2 and 5 mV at pH 2.8 and 2, respectively [39]. This membrane is suitable for operation at pH from 2 to 11 up to a maximum pressure and temperature of 41 bar and 45 °C, respectively. HydraCoRe 70pHT is based on a sulfonated polyethersulfone active layer. Coatings of sulfonated polysulfone or sulfonated polyethersulfone have been applied to a porous support to create negatively charged membranes (due to the presence of $R-SO_3H$ groups) with good chemical resistance to acids and chlorine [40–42]. According to literature, HydraCoRe 70pHT is a negatively charged membrane with zeta potential value constant (-85 mV) for the pH range from 3 to 11 [43]. Breite et al. [44] also reported negative values of z-potential from pH 3 to 11 for synthetized membranes containing sulfonic groups. In addition, membranes containing sulfonic groups (widely used in electrodialysis and diffusion dialysis) have pKa values between 0 and 1 [45]. Thus it was expected qualitatively that at the acidity conditions in this study (pH of 2.0 and 2.8) the membrane was negatively charged [45]. HydraCoRe membrane allows operation at a wider range of pH, with values lying between 1 and 13.5 and maximum temperature and pressure of 70 °C and 41 bar, respectively. HydraCoRe 70pHT membrane is suitable for color removal. Nevertheless, the presence of a high negative surface charge might make this membrane suitable for acid removal too. Figure 1 shows the chemical active layer of both membranes.

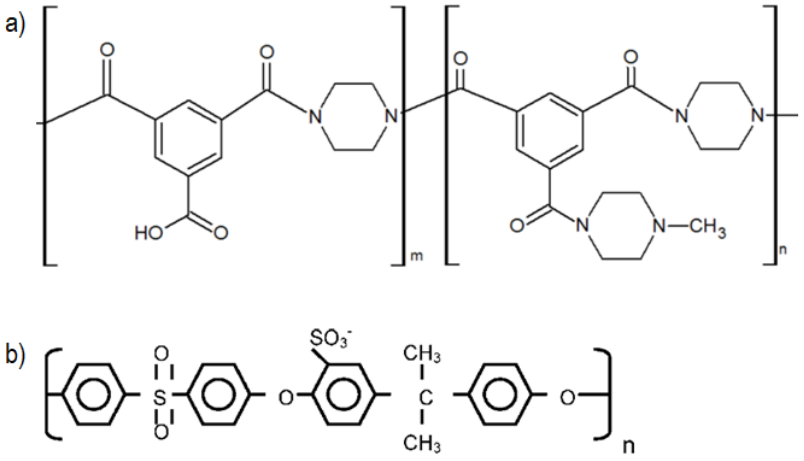

Figure 1. Chemical structure of a) NF270 [45] **and b) a sulfonated polyethersulfone** [46]

Feed solution (50 L) was kept in a refrigerated tank at 25 ± 2 °C and was pumped to the membrane module by a diaphragm pump, passing previously through a pre-filter cartridge. The solution reached the membrane module and two output streams were obtained, the permeate and the retentate. Both generated streams (retentate and permeate) were recirculated to the feed tank solution. In order to control the trans-membrane pressure (TMP) and cross-flow velocity (cfv), one by-pass valve before the entrance of the module and a needle valve in the retentate stream were used. These two valves allowed to vary the TMP, which was directly correlated with the trans-membrane flux. Several parameters such as pressure, conductivity and flow-rate were monitored during the experiments by means of manometers, conductivity-meters and flow-meters. NF270 and HydraCoRe 70pHT modules had an active area of 2.6 m^2 and 6.4 m^2, respectively. Figure 2 shows a scheme of the experimental setup used.

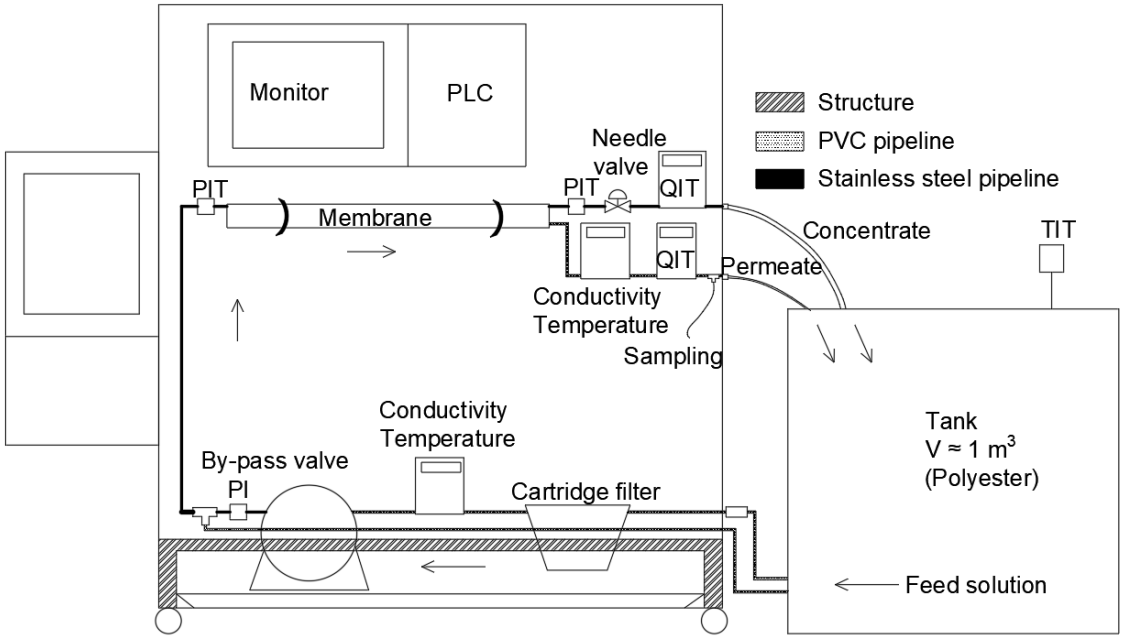

Figure 2. Experimental setup for the SW membrane configuration including details on the main system components (feed solution tank, membrane module, pump, on-line monitoring sensors (T, P, electric conductivity) and piping). Arrows indicate fluid circulation directions.

The experimental procedure started with the membrane compaction at 20 bar for 2 hours by filtering feed solution. After that, feed flow rate was fixed at 14.3 L/min and pressure was gradually varied from 4.5 to 20 bar. Samples from the permeate side were collected and analyzed at different TMP. Once an experiment was finished, the membrane was cleaned with de-ionized water at 10 bar for 1 h and at 20 bar for 1.5 h. To ensure that the membrane was cleaned successfully, the hydraulic permeability was compared with the corresponding value of a virgin membrane. If both values differed by more than 5 %, another cleaning was applied again until differences were below that value.

A second set of experiments was carried out in order to simulate filtration in a vessel containing six spiral wound membrane modules. For this purpose, the two output streams generated by the module were collected in different tanks, and only the concentrate collected from one step was

used as feed solution for the next one. Before filtering the concentrate in the next membrane step, solution was allowed to circulate through the system for 5 minutes. TMP was fixed at 10 bar, which was the TMP at which maximum rejections were observed in the first set of experiments. Concentrate and permeate samples were collected and analysed in each membrane filtration step.

2.3. Analytical methods

Samples were analyzed by different techniques, depending on the ion of interest. Sodium and sulfate were analyzed by ion-chromatography (Dionex ICS-1000 and Dionex ICS-1100). Two different columns were used: IONPAC® CS16 and IONPAC® AS23 for cations and anions, respectively. Cationic exchange column used 0.03 mol/L methane sulfonic acid as eluent, while anionic exchange column used a mixture of 4.5 mmol/L Na_2CO_3 and 0.8 mmol/L $NaHCO_3$ as eluent. The pH of feed and permeate solutions were measured with a pH electrode. Copper and zinc were analyzed by atomic absorption spectrophotometry (VARIAN SPECTRAA-640), and Fe(II) concentration was determined by an acid-base titration (Mettler Toledo T70), using a Pt electrode and potassium dichromate ($K_2Cr_2O_7$) 0.01 mol/L as titrant solution.

The analytical techniques used in this study allowed to measure the total concentration values of each element (e.g., Na and SO_4). Then, from the chemical equilibrium reactions constants it is possible (Table A1.1 in Annex I) to determine the free concentration values of the different ions in solution (e.g, Na^+, $NaSO_4^-$, HSO_4^-). Then, under this scenario and due to the difficult to describe the solution-chemistry inside the membrane free-volume, the ion rejections were described according the predominance of the dominant ions.

2.4. Ion rejection modelling by using the Solution-Electromigration-Diffusion-Film model

Solution-Electromigration-Diffusion-Film model was applied to fit experimental data for both dominant salt and trace ions [32,34,35,47]. The dominant salt is formed by the cation and anion with the highest concentration in solution. Trace ions are defined as those whose concentration is lower than 5 % of the concentration of the dominant salt. In our experiments, the dominant salt was Na_2SO_4, while the trace ions were H^+ and, when present, Cu^{2+} and Zn^{2+}. It is worth to mention that Fe^{2+}, when present, had a concentration comparable to that of the dominant salt and, therefore, it could not be considered a trace ion. The model allows to relate the observable (R^{obs}) and intrinsic (R^{int}) rejections of the dominant salt and trace ions as a function of trans-membrane flux (J_v). Intrinsic rejection takes into account the ion concentration in the solution adjacent to the membrane surface due to concentration polarization, while observable rejection is referred to feed solution concentration (see Eqs. 2 and 3). It must be bear in mind that the applicability of the model is limited to the presence of only one dominant salt. Therefore, while the model could be applied in those experiments with a feed solution containing only the dominant salt (Na_2SO_4), it could not be applied in those others with a feed solution containing also Fe^{2+} at a concentration comparable to that of Na_2SO_4.

Equations from the model are collected in Table 2. Concentrations of dominant salt and trace ion are referred in equations as c_s and c_t, respectively. Subscripts identifies the feed (c') and permeate side (c''), while $c^{(m)}$ is referred to the ion concentration in the solution adjacent to the membrane surface. First of all, the fitting of the dominant salt is performed (Eq. 1) to determine two parameters: the permeances of the membrane and the concentration polarization layer to the dominant salt (P_s and P_s^{δ}). These parameters allow to determine the thickness of the unstirred layer (δ). Intrinsic rejection of dominant salt (R_s^{int}) can be calculated by Eq. 6 and its reciprocal intrinsic transmission (f_s). The concentration of trace ions in the solution adjacent to the

membrane surface can be calculated by Eq. 8 and, then, its intrinsic rejection (R_t^{int}) and reciprocal intrinsic transmission (f_t) can be determined. From Eq. 13 and f_t, the parameters b and K are calculated and used for the determination of the membrane permeances to dominant and trace ions ($P_{\pm}$, P_t) following Eq. 17 and Eq. 18 .

Table 2. Transport equations of SEDF model [32,34,35,47]

Observable salt rejections	
$R_s^{obs} = \frac{\frac{J_v}{P_s}\exp\left(-\frac{J_v}{P_s^{(\delta)}}\right)}{1+\frac{J_v}{P_s}\exp\left(-\frac{J_v}{P_s^{(\delta)}}\right)} R_s^{obs} = \frac{\frac{J_v}{P_s}exp\left(-\frac{J_v}{P_s^{(\delta)}}\right)}{1+\frac{J_v}{P_s}exp\left(-\frac{J_v}{P_s^{(\delta)}}\right)}$ Where:	Eq. 1
$R_s^{obs} \equiv 1 - \frac{c_s^{"}}{c_s^{'}}$	Eq. 2
$R_s^{int} \equiv 1 - \frac{c_s^{(m)}}{c_s^{'}}$	Eq.3
$P_s^{(\delta)} = \frac{D_s^{(\delta)}}{\delta}$	Eq. 4
$D_s^{(\delta)} = \frac{(Z_+ - Z_-)D_+^{(\delta)}D_-^{(\delta)}}{Z_+D_+^{(\delta)} - Z_-D_-^{(\delta)}}$	Eq. 5
Intrinsic salt rejections	
$R_s^{int} = \frac{\frac{J_v}{P_s}}{1+\frac{J_v}{P_s}}$ Where:	Eq. 6
$R_s^{int} \equiv 1 - \frac{c_s^{"}}{c_s^{(m)}}$	Eq. 7
Trace ion concentration in the solution adjacent to the membrane surface	
$\frac{c_t^{(m)}}{c_t^{'}} =$	Eq. 8

$$exp\left(Pe_t\right)[1+R_s^{obs}(exp(Pe_s)-1)]^{b^{(\delta)}}\cdot$$

$$\left\{1-\left(1-R_t^{obs}\right)\int_{exp\left(-Pe_t\right)}^{1}\frac{dy}{\left[1+R_s^{obs}(y^{-\alpha}-1)\right]^{b^{(\delta)}}}\right\}$$

Where:

$$Pe_t = \frac{J_v\cdot\delta}{D_t^{(\delta)}} \quad \text{Eq. 9}$$

$$Pe_s = \frac{J_v\cdot\delta}{D_s^{(\delta)}} \quad \text{Eq. 10}$$

$$b^{\delta} \equiv \frac{Z_t\cdot(D_+^{(\delta)}-D_-^{(\delta)})}{Z_+D_+^{(\delta)}-Z_-D_-^{(\delta)}} \quad \text{Eq. 11}$$

$$\alpha = \frac{D_t^{(\delta)}}{D_s^{(\delta)}} \quad \text{Eq. 12}$$

Reciprocal transmission of trace ion

$$f_t = (f_s)^b + K\cdot\left(\frac{f_s-(f_s)^b}{1-b}\right) \quad \text{Eq. 13}$$

Where:

$$f_s = \frac{c_s^{(m)}}{c_s^{"}} = \left(\frac{1}{1-R_s{}^{int}}\right) \quad \text{Eq. 14}$$

$$f_t = \frac{c_t^{(m)}}{c_t^{"}} = \left(\frac{1}{1-R_t{}^{int}}\right) \quad \text{Eq. 15}$$

$$b \equiv \frac{Z_t\cdot(P_+-P_-)}{Z_+P_+-Z_-P_-} \quad \text{Eq. 16}$$

$$K \equiv \frac{P_s}{P_t} \quad \text{Eq. 17}$$

Membrane permeances to dominant ions

$$P_{\pm} = \frac{P_s}{1-\left(\frac{Z_{\pm}}{Z_t}\right)\cdot b} \quad \text{Eq. 18}$$

3. Results and discussion

3.1. Rejection of Na_2SO_4 from solutions at acidic pH (2.0 to 2.8)

The observable rejections for the dominant salt (Na_2SO_4) and trace ion (H^+) as a function of trans-membrane flux for both membranes (NF 270 and HydraCoRe 70pHT) at pH 2.8 and 2.0 are depicted in Figure 3. Symbols represent the experimental data and lines are the SEDF model prediction (equations were shown in Table 2). From the measured concentrations of Na^+ and SO_4^{2-} in feed and permeate streams, the rejection of each ion was calculated. Due to the low concentration of H^+ in solution, both ions (Na^+ and SO_4^{2-}) permeated together to ensure electro-neutrality and the differences between their rejections were lower than 1 %. Na_2SO_4 rejection depicted in the Figure 3 was calculated as the mean of Na^+ and SO_4^{2-} rejections.

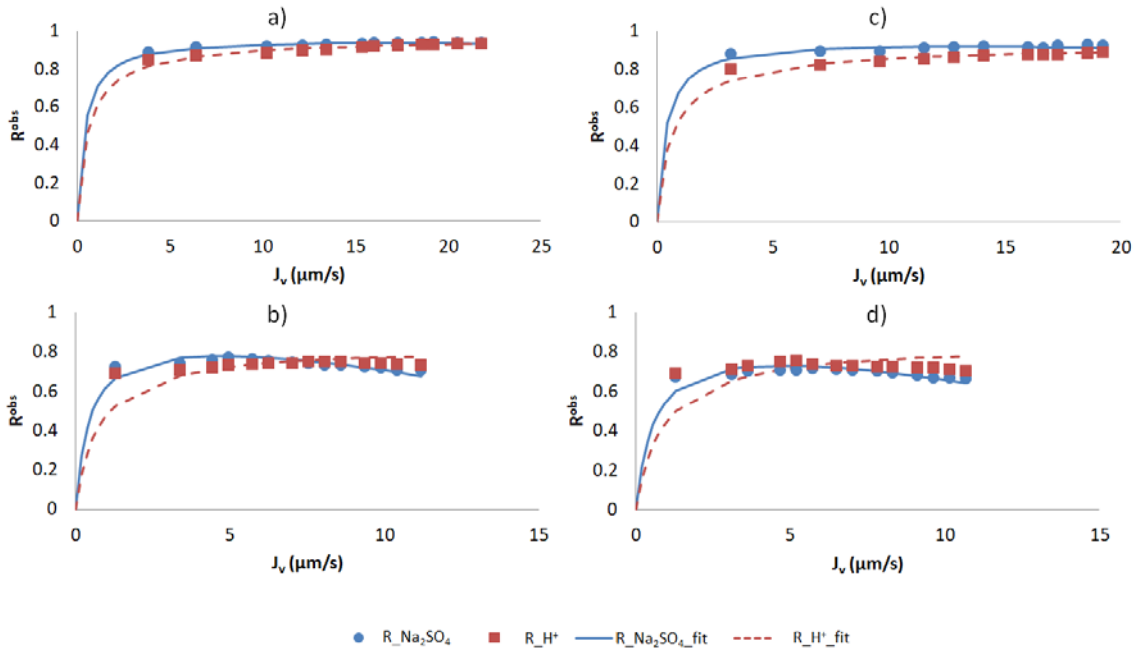

Figure 3. Observable rejection (R^{obs}) curves as a function of trans-membrane flux (J_v) with feed solution containing sodium sulfate (Na_2SO_4) at pH 2.8 for a) NF270 and b) HydraCoRe 70pHT membranes, and at pH 2.0 for c) NF270 and d) HydraCoRe 70pHT membranes. Points and lines represent the experimental data and prediction by SEDF model, respectively.

Both membranes exhibited different performance due to differences in their active layer properties. First, NF270 allowed to obtain higher trans-membrane fluxes than HydraCoRe 70pHT for the same TMP (Table 3). Second, NF270 showed Na_2SO_4 rejection higher than 89 % for both pH 2.8 and 2.0, while in the case of HydraCoRe 70pHT the rejection was around 75 %.

Table 3. Trans-membrane pressure and corresponding pH and solvent flux of permeate stream for NF270 and HydraCoRe 70pHT membrane with Na_2SO_4 solutions

	NF270				HydraCoRe 70pHT			
	Feed pH = 2.8		Feed pH = 2.0		Feed pH = 2.8		Feed pH = 2.0	
ΔP (bar)	Jv (μm/s)	Permeate pH	Jv (μm/s)	Permeate pH	Jv (μm/s)	Permeate pH	Jv (μm/s)	Permeate pH
8.35	3.8	3.8	3.2	2.9	3.4	3.5	3.1	2.8
11.5	12.2	3.9	11.5	3.0	5.7	3.6	5.2	2.9
15.5	17.3	4.1	16.6	3.1	8.1	3.6	7.8	2.8
20	21.8	4.1	20.5	3.2	11.2	3.6	10.6	2.8

Ion rejection depends not only on the type of membrane used as shown in Figure 3 but, for a given membrane, also on the pH. This influence of pH was reported by Artuğ et al. [48], who evaluated a number of different commercial NF membranes, including NF270, in a cross-flow filtration under flat sheet configuration and observed a decrease of Na_2SO_4 rejection from 98% to 90% when pH was lowered from 6 to 2.5. This decrease was attributed to a change of the membrane charge, which shifted from negative at pH 6 to positive at pH 2.5. According to literature, the IEP of the NF270 membrane lies between 2.5 and 3.5, depending on the electrolyte and its concentration [24,48]. Therefore, it is expected that at pH lower than the IEP, the

membrane becomes positively charged due to the protonation of carboxylic groups (R-COOH) and to the partial protonation of amine groups ($R\text{-}NH_3^+$).

Together with the membrane charge, equilibrium reactions among the different ion species in solution should also be considered. As shown by the speciation diagrams in Annex I, SO_4^{2-} is not the only anion species present at pH 2.8, since it co-exists with HSO_4^- and $NaSO_4^-$ (which represent 10% and 20% of the total sulfate in solution, respectively). Thus, speciation is of paramount importance, since not all species are equally transported through (and therefore equally removed by) a membrane. According to the dielectric exclusion phenomenon [49], the transport of single-charged ions (such as HSO_4^- and $NaSO_4^-$) is favored over that of multi-charged ions (such as SO_4^{2-}). Moreover, according to Donnan exclusion, transport of counter-ions is favored through the membrane, while the passage of co-ions is impeded. Nevertheless, despite the electrostatic repulsion between counter-ions and the membrane fixed charges, an equal number of counter-ions permeate through the membrane to meet electro-neutrality requirement. Figure 4 illustrates the effect of pH on the transport of ions through the NF270 membrane. These factors explain why salt rejection by NF270 slightly decreased from 89% to 87% when pH was lowered from 2.8 to 2.0 (Figure 3). On the one hand at pH 2.0, SO_4^2 partially shifted to HSO_4^- (showing a prevalence of 40% of the total sulfate, see Annex I) and to $NaSO_4^-$ (around 20 % of total sulfate), which better permeate through the membrane than SO_4^{2-}. On the other hand, lowering pH from 2.8 to 2.0 resulted in a more positively charged membrane (z-potential increased from 2 to 5 mV when pH was decreased [39]), which further favored the passage of HSO_4^- and $NaSO_4^-$ through the membrane. Proton rejection also decreased. Transport of H^+ was favored instead of Na^+ due its lower size and higher diffusivity. Due to the positive membrane charge, the dominant ion in solution (Na^+) controlled the transport of ions through the membrane. Visser et al. [25] filtered acidic Na_2SO_4 solutions ($5 \cdot 10^{-3}$ M) with different

NF membranes in a dead-end module and reported that Na_2SO_4 rejection decreased when pH was lowered due to the presence of single-charged HSO_4^-.

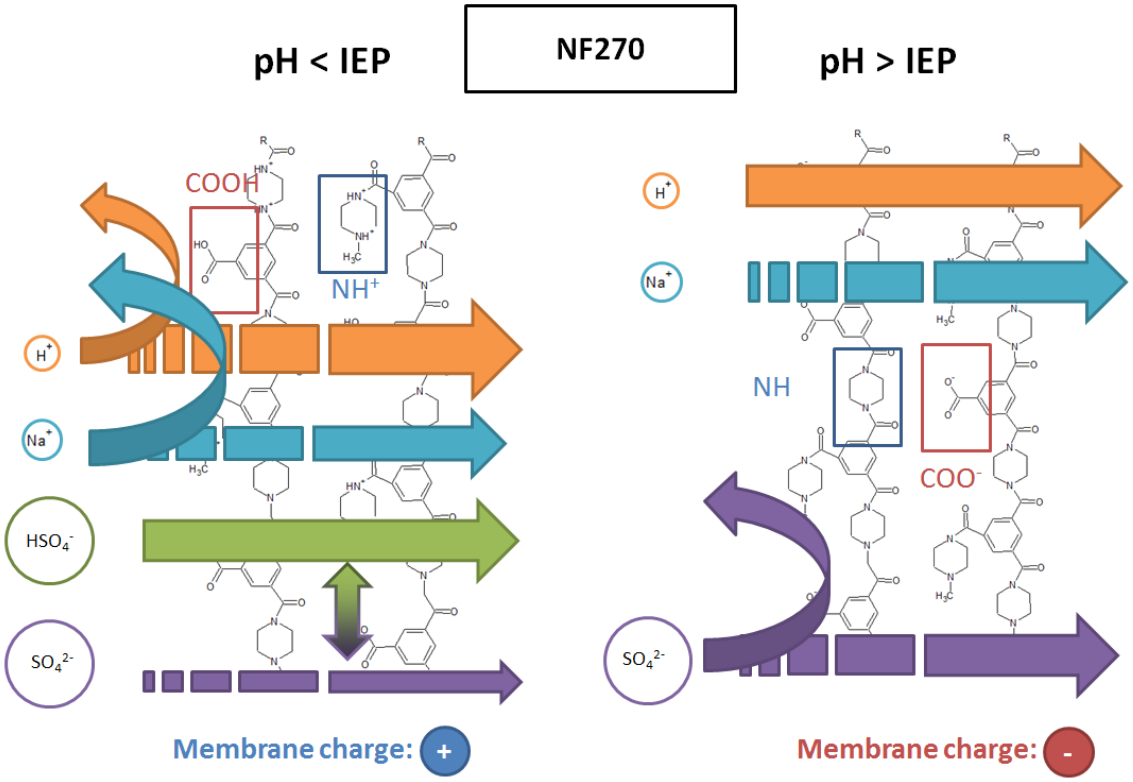

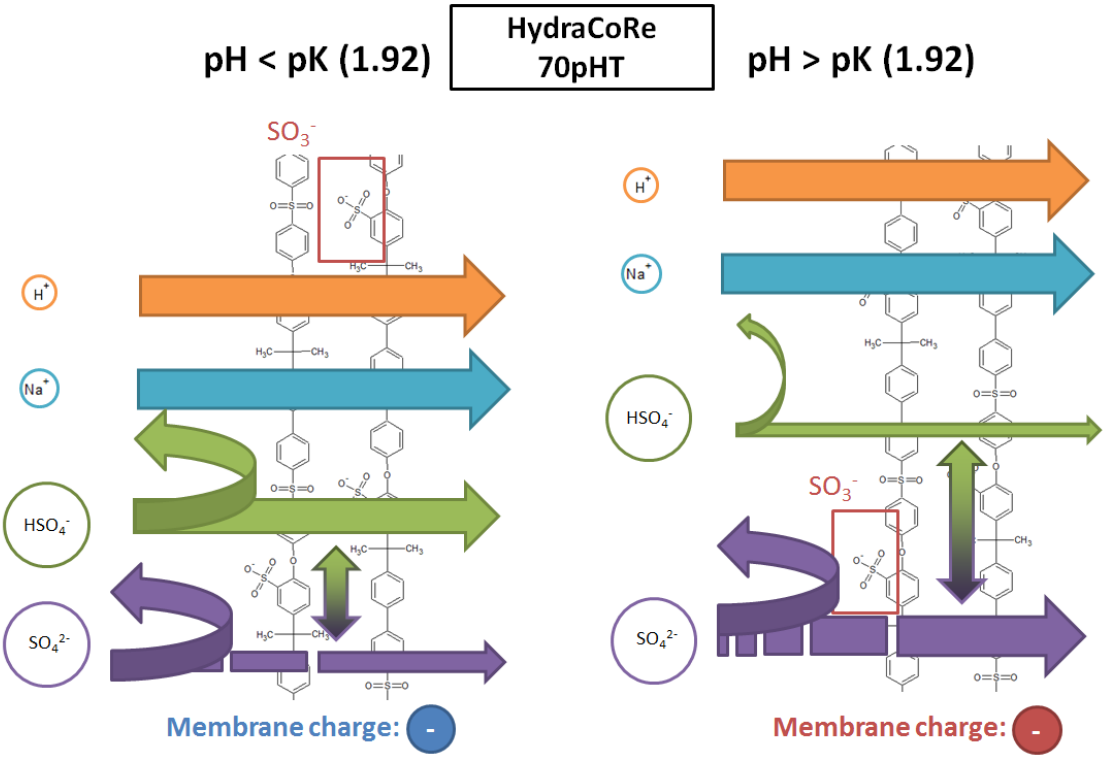

Figure 4. Schematic representation of the ion transport (expressed by arrows) depending on pH for NF270 and HydraCoRe 70pHT membranes.

Na_2SO_4 rejection for HydraCoRe 70pHT decreased from 75 % (pH 2.8) to 70% (pH 2.0). Similarly to the NF270 membrane trend, the charge of the HydrCoRe 70pHT membrane is affected by pH solution though in a different way. At both pH (2.8 and 2.0), this membrane is expected to be negatively charged, due to the presence of ionized sulfonic groups ($R\text{-}SO_3^-$). As reported in the literature, HydraCoRe 70pHT contains a negatively charged active layer with zeta potential value constant (-85 mV) for the pH range from 3 to 11 [43]. According to ion-exchange membranes data, the pK_a values for sulfonic groups lies in between 0 and 1, thus it is expected that at the evaluated pH range (2 to 2.8) the membrane is negatively charged [50]. Figure 4 illustrates the effect of pH in relation to the pK_a value of HSO_4^-/SO_4^{2-} equilibrium on the transport of ions through the HydraCoRe 70 pHT membrane. The negative charge at pH 2.8 impedes the passage of SO_4^{2-} (predominant species accounting for approximately 70% of the total sulfate as shown in Appendix I). However, at pH 2.0 the transport of species HSO_4^- and $NaSO_4^-$ (which together account for around 60% of the total sulfate) was favored, leading to lower rejections, despite the negative membrane surface charge. Proton rejections slightly decreased when pH was lowered. For this membrane, rejections reached a maximum at trans-membrane flux of approximately 5 μm/s and started to decrease at higher trans-membrane fluxes. This behavior might be related to the concentration polarization [51,52]. The decrease in ion rejection was caused by a low mass transfer coefficient inside the module, leading to a higher ion concentration in the nearby of the membrane. Therefore, there was a higher concentration difference between both sides of the membrane that led to lower observable rejection values. No data of Na_2SO_4 rejection for HydraCoRe 70pHT was found in literature for comparison.

The membrane permeances to ions are collected in Table 4. These values were in agreement with the dielectric exclusion phenomena [49], by which the membrane permeance to an ion

312 decreases as the absolute value of the charge of the ion increases, e.g., membrane permeance
313 to SO_4^{2-} was much lower than to Na^+ and H^+. For NF270, an increase in membrane permeance to
314 SO_4^{2-} was observed when pH was lowered, caused by the shift of SO_4^{2-} to HSO_4^-. Due to the
315 higher positive membrane charge at pH 2.0 (5 mV instead of 2 mV, [39]) a decrease in
316 membrane permeance to Na^+ was observed, while for H^+ an increase of its value was noticed
317 due to lower electrostatic repulsion between the ion and the membrane. Published studies
318 reported similar values of NF270 membrane permeances to ions under FS and SW
319 configurations [32,34,35,47,53]. Reig et al. [53] filtering Na_2SO_4 solutions at neutral pH with
320 NF270 membrane under FS and SW configurations, determined membrane permeances to Na^+
321 of >60 µm/s (higher than in the present study) and to SO_4^{2-} in the range of 0.03-0.12 µm/s (lower
322 than in the present study). No data were published for H^+. These differences can be attributed to
323 the lower pH (2.0 and 2.8) of the present study than in the mentioned previous studie (neutral
324 pH). At neutral pH carboxylic groups of NF270 are expected to be ionized ($R\text{-}COO^-$), thus leading
325 to a negative surface charge. When pH is lowered carboxylic groups and amine groups get
326 protonated (R-COOH and $R\text{-}NH_2^+$), leading to a positive surface charge. This implies that Na^+ will
327 suffer an electrical repulsion, while SO_4^{2-} will pass easily at acidic pH.
328 For HydraCoRe 70pHT membrane, the decrease in pH led to an increase of membrane
329 permeance to ions in solution, e.g., membrane permeance to Na_2SO_4 increased from 0.5 to 0.7
330 µm/s when pH was lowered from 2.8 to 2.0. As mentioned above, the most favored ion to
331 permeate through the membrane is H^+ because of its size and higher diffusivity. Calculated
332 values of membrane permeance to H^+ were in agreement with this fact, as they were more than
333 100 times higher than the permeance to Na^+. The shift of SO_4^{2-} to HSO_4^- at lower pH resulted in
334 an increase of the membrane permeance to sulfate from 0.22 to 0.28 µm/s, when pH was
335 lowered from 2.8 to 2.0.

A comparison of membrane permeances to ions between the two membranes showed that HydrCoRe 70pHT generally presented higher membrane permeances than NF270. For instance, at pH 2.0, membrane permeances to dominant salt (Na_2SO_4) and SO_4^{2-} were 0.7 μm/s and 0.28 μm/s, respectively, while they were 0.4 μm/s and 0.18 μm/s, respectively, for NF270.

Table 4. Concentration polarization and membrane permeances to Na_2SO_4 (P_s and $P_s\delta$), and membrane permeances to Na^+, SO_4^{2-} and H^+ for NF270 and HydraCoRe 70pHT membrane under SW configuration at pH 2.8 and 2.0

pH	Permeance to salt, Na_2SO_4 (μm/s)		Membrane permeance to ion (μm/s)		
	$P_s^{(\delta)}$	P_s	Na^+	SO_4^{2-}	H^+
NF270					
2.8	17.0	0.4	1.7	0.17	422.0
2.0	12.8	0.4	1.2	0.18	410.3
HydraCoRe 70pHT					
2.8	4.7	0.5	1.2	0.22	486.6
2.0	4.8	0.7	1.9	0.28	653.6

3.2. Rejection of metallic ions (Fe^{2+}, Zn^{2+} and Cu^{2+}) in Na_2SO_4/H_2SO_4 solutions at acidic pH (2 to 2.8)

Figure 5 shows the rejection of all the elements for both membranes when a synthetic AMD was filtered at pH 2.8 and 2.0. Figures 5a and 5c represent the experimental data for NF270 and Figures 5b and 5d the data for HydraCoRe 70pHT.

NF270 showed high rejection for the metallic ions in solution (>90 % at pH 2.8 (Figure 5a) and >95 % at pH 2.0 (Figure 5c)). These rejection values increased with trans-membrane flux and concentration polarization was not observed along the flux range. For both pH conditions rejection followed the trend $R(Fe^{2+}) \approx R(Zn^{2+}) \approx R(Cu^{2+}) > R(Na^{+}) > R(H^{+})$, according to dielectric exclusion [49]. Differences in cations rejections could be related to differences in ion diffusivities inside the membrane. An increase in rejection was mainly caused by the positive membrane charge, as explained in section 3.1. At pH 2.0 the membrane was more positively charged and the passage of cations through it was impeded, thus leading to a lower rejection of H^{+} (higher ion diffusivity than Na^{+} and metallic ions).

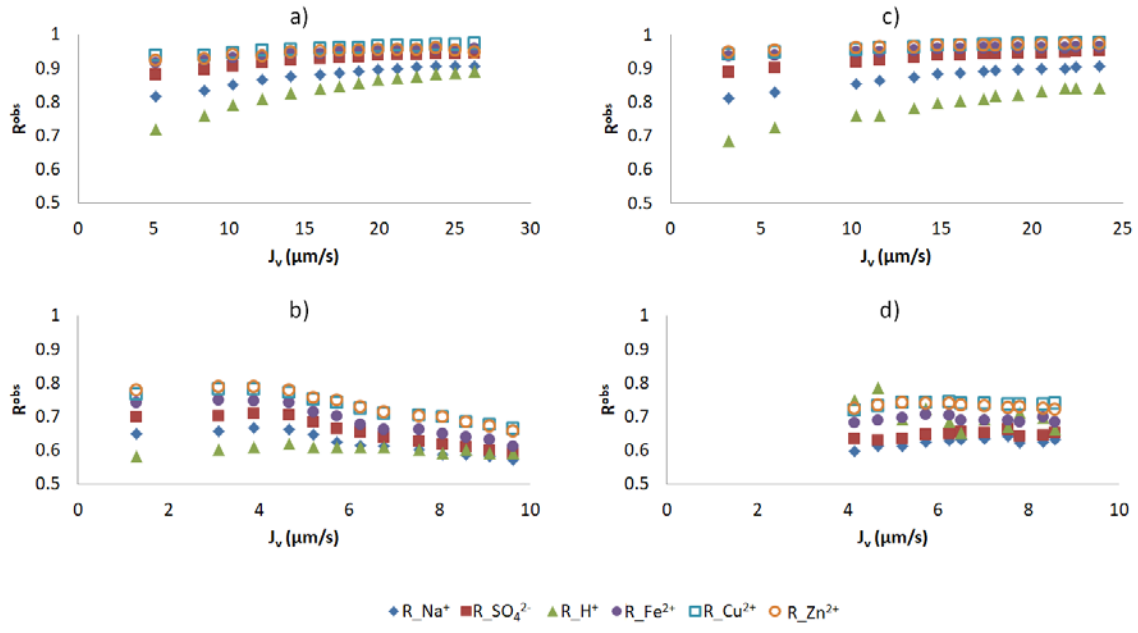

Figure 5. Observable rejection (R^{obs}) curves as a function of trans-membrane flux (J_v) with feed solution mimicking AMD at pH 2.8 for a) NF270 and b) HydraCoRe 70pHT membranes, and at pH 2.0 for c) NF270 and d) HydraCoRe 70pHT membranes.

Rejections for all ions were lower for the HydraCoRe 70pHT membrane than for the NF270 membrane because of the negative charge of the former, which favored the transport of cations

through the membrane. For this membrane, rejections for all species at pH 2.8 (Figure 5b) were approximately constant at volumetric trans-membrane fluxes below 5 μm/s. From this flux onward, rejections gradually decreased due to concentration polarization. Rejections of double-charged metals were around 75 % for the first trans-membrane fluxes and decreased to 65 %. When pH was decreased to 2.0 (Figure 5d), rejections for all the species in solution also decreased. At this pH the membrane was still negatively charged, but the concentration of HSO_4^- (which is less affected by dielectric exclusion and therefore its permeance through the membrane is favored) was higher than that of SO_4^{2-}, resulting in lower sulfate rejections. The presence of this single-charged anion made cations rejection decrease. At the first trans-membrane flux values, metallic ions rejections were around 70 %, and in this case no concentration polarization was observed. For both cases, rejection for cations followed the previous trend: $R(Fe^{2+}) \approx R(Zn^{2+}) \approx R(Cu^{2+}) > R(Na^+) > R(H^+)$.

From a hydraulic point of view, NF270 showed a better performance under the tested conditions, achieving higher permeate fluxes and rejections for the same applied pressure than HydraCoRe 70pHT (Table 5).

Results showed that both membranes allow to concentrate metallic species in the retentate stream, specially the NF270 membrane. A diluted stream of sulfuric acid is recovered in the permeate. The concentration factor on the retentate stream can be enhanced if AMD is treated sequentially by a series of NF steps.

Table 5. Trans-membrane pressure and corresponding pH and solvent flux of permeate stream for NF270 and HydraCoRe 70pHT membrane with Na_2SO_4 solutions containing metallic ions

	NF270				HydraCoRe 70pHT			
	pH = 2.8		pH = 2.0		pH = 2.8		pH = 2.0	
ΔP (bar)	Jv (µm/s)	Permeate pH	Jv (µm/s)	Permeate pH	Jv (µm/s)	Permeate pH	Jv (µm/s)	Permeate pH
8.35	10.2	3.48	10.3	2.94	1.3	3.20	1.3	2.55
10.5	14.1	3.56	13.5	2.98	3.9	3.23	4.1	2.70
14.7	19.9	3.67	17.9	3.06	6.8	3.23	6.5	2.56
19.7	26.3	3.76	23.7	3.12	9.6	3.21	8.6	2.57

3.3. Metal and sulfate recovery and concentration factors in acidic mine waters.

A full-scale vessel was simulated with the bench-scale NF module by recirculating and filtrating the concentrate stream sequentially in 6 steps (Figure 6). This experiment was performed with both membranes and with the synthetic AMD (i.e. including double-charged metals) at pH 2.8. From the experiments performed in sections 3.2, a pressure of 10 bar was selected for two reasons: i) ion rejection barely increased at higher TMP for both membranes and ii) concentration polarization phenomena was avoided for HydraCoRe 70pHT. Table 6 collects the concentrations of feed solution, as well as the rejection of the different species for each filtration step.

Table 6. Concentration of the ions in the feed and rejection achieved in each membrane step.

	NF270						HydraCoRe 70pHT					
	pH	$[Na^+]$ (mg/L)	$[SO_4^{2-}]$ (mg/L)	$[Fe^{2+}]$ (mg/L)	$[Zn^{2+}]$ (mg/L)	$[Cu^{2+}]$ (mg/L)	pH	$[Na^+]$ (mg/L)	$[SO_4^{2-}]$ (mg/L)	$[Fe^{2+}]$ (mg/L)	$[Zn^{2+}]$ (mg/L)	$[Cu^{2+}]$ (mg/L)
Feed	2.95	1400	9950	4330	380	172	2.86	1180	7920	3610	333	314
Rejection												
	NF270						HydraCoRe 70pHT					
	H^+	Na^+	SO_4^{2-}	Fe^{2+}	Zn^{2+}	Cu^{2+}	H^+	Na^+	SO_4^{2-}	Fe^{2+}	Zn^{2+}	Cu^{2+}
Mem. 1	78.6	87.1	91.6	92.7	93.7	92.0	51.0	57.7	59.2	60.7	64.9	66.4
Mem. 2	76.6	86.2	90.9	91.8	92.9	89.6	48.7	53.8	54.3	58.9	62.6	63.9
Mem. 3	75.5	84.3	90.0	90.9	92.4	89.2	46.3	50.1	49.7	55.7	59.3	61.4
Mem. 4	74.9	82.7	88.3	90.2	91.7	88.3	47.5	45.7	45.1	48.2	55.9	58.0
Mem. 5	74.3	80.9	86.5	88.2	90.6	86.9	46.3	42.4	41.0	44.0	53.0	56.2
Mem. 6	73.7	77.7	83.9	87.0	89.1	86.1	47.5	37.8	36.8	39.9	48.0	52.2

For NF270 double-charged metal cations and sulfate were rejected by more than 90 % in the first filtration step, and the rejection value gradually decreased down to 84-89% in the last filtration step. Proton rejections also decreased after each step. The fact that solution became concentrated led to an increase of diffusive forces in the separation process and, then, to lower rejections. At the end of the process, concentration factor for all the metals in solution was around 2. Concentration factor was defined as the ratio between the concentration of ion *i* at the end of the process (i.e. in the concentrate stream obtained after the sixth step) relative to that in the feed stream.

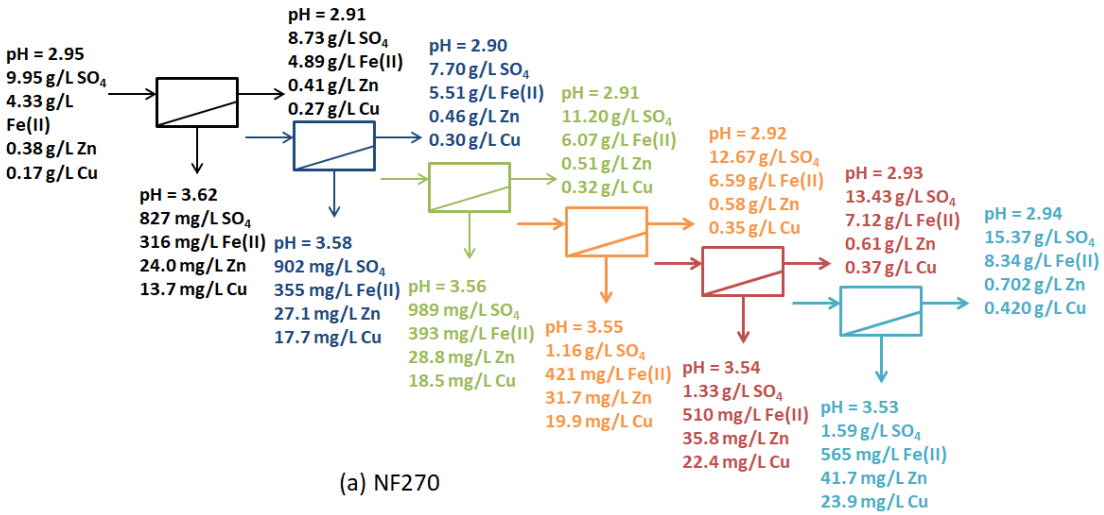

(a) NF270

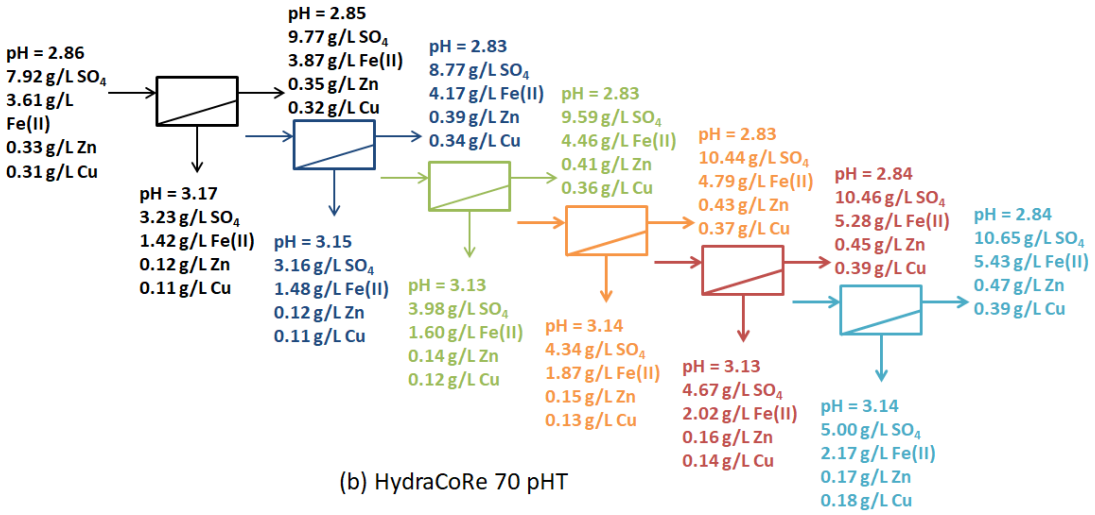

(b) HydraCoRe 70 pHT

Figure 6. Details on the variation of the total concentration of the main components (SO_4^{2-}, Fe^{2+}, Zn^{2+} and Cu^{2+}) and pH along a series of 6 membrane steps at TMP of 10 bar at pH 2.8 for (a) NF270 and (b) HydraCoRe 70pHT

For HydraCoRe 70pHT, metallic ion rejections were all between 61-66% in the filtration steps. At pH 2.8, HydraCoRe 70pHT membrane presented a strong negative charge, resulting in low cation rejections. Along the whole process, rejections for all the elements in solution decreased, due to higher diffusive forces in the separation process and proton rejections also decreased. In the overall process metal ions were concentrated by 50%.

Experiments simulating AMD filtration through a full-scale vessel containing 6 spiral wound membrane modules were not performed at pH 2.0, but the performance of both membranes at this pH was estimated by applying mass balances assuming that the rejections were the same as those obtained in the single-step experiments at pH 2.0 discussed at section 3.2 and shown in figure 5. Figure 7 shows the calculated ion concentrations in each step for both membranes.

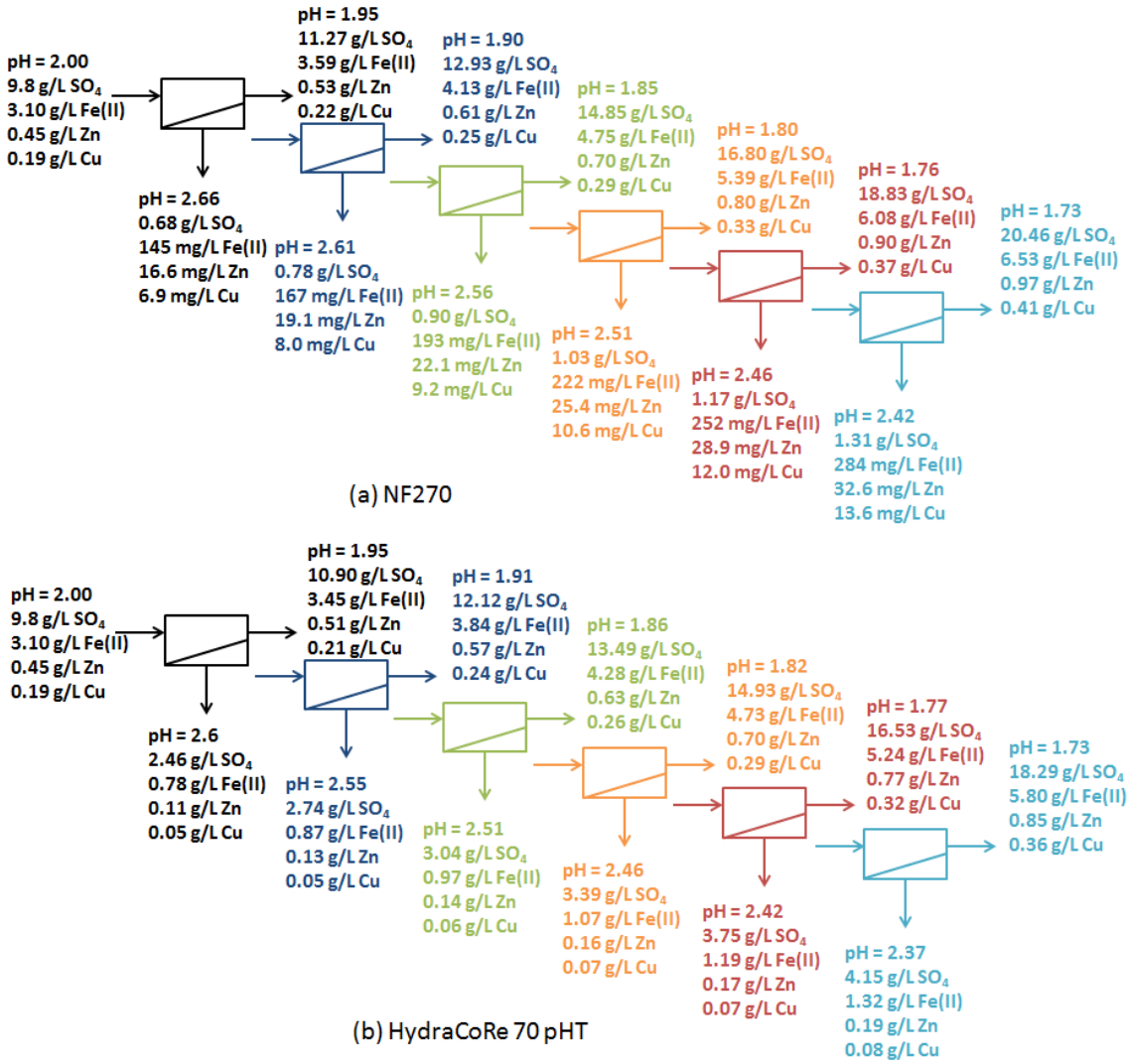

Figure 7. Details of the variation of the total concentration of the main components (SO_4^{2-}, Fe^{2+}, Zn^{2+} and Cu^{2+}) and pH for a feed stream at pH 2.0 for (a) NF270 and (b) HydraCoRe 70pHT. Values were calculated taking into account data from the single step filtration in section 3.2.

Results showed that both membranes would allow to obtain an acidic stream containing sulfuric as permeate and a stream rich in metallic ions as concentrate. NF270 membrane provided a permeate with a lower concentration of H_2SO_4 (but also of Fe(II) as impurity), while the HydraCoRe 70pHT provided a permeate with a higher concentration of H_2SO_4 (but also of Fe(II) as impurity).

With regard to the concentrate stream, the concentration factors for the double-charged metal ions were around 2 and 1.5 for the NF270 and HydraCoRe 70pHT membranes, respectively. These concentration factors were moderate and similar for all the studied metals (Fe^{2+}, Zn^{2+} and Cu^{2+}), resulting in a limited selectivity and indicating that a post-treatment is needed for the separation and recovery of these metals. This post-treatment can be based on oxidation of Fe^{2+} to Fe^{3+} and subsequent removal of Fe^{3+} 1) by precipitation as $Fe(OH)_3(s)$ at pH 3 (but at the expenses of hindering sulfuric acid recovery), or 2) by NF unit, followed by an ion-exchange step using a Cu/Zn selective impregnated resin.

4. Conclusions

Polyamide-based NF membrane (NF270) showed a better performance (higher trans-membrane fluxes and rejections) than sulfonated polyethersulfone-based one (Hydracore 70pHT) for AMD treatment. NF270 allowed to obtain rejection values higher than 90 % for SO_4^{2-} and for double-charged metals (Fe^{2+}, Zn^{2+} and Cu^{2+}), while HydraCore 70pHT showed rejection values around 75 %, which decreased at higher trans-membrane fluxes due to concentration polarization phenomena. When pH was lowered from 2.8 to 2.0 SO_4^{2-} shifted to HSO_4^- and $NaSO_4^-$, which were less affected by dielectric exclusion than SO_4^{2-}, resulting in a lower rejection of total sulfate for both membranes. Another factor that must be taken into account in the separation process is the membrane charge. At the typical pH range of AMD, NF270 has a positive charge (because carboxylic and amine groups are fully and partially protonated, respectively), while HydraCoRe

70pHT has a negative surface membrane charge (because sulfonic groups are fully dissociated). This negative charge provides HydraCoRe 70pHT of permanent ionized groups, exhibiting a behavior approaching an ion-exchange membrane. Then, ion transport is more influenced by the presence of these groups, favoring the transport of single-charged cations. However the differences in selectivity of the sulfonated membrane, between single-charged (Na^+, H^+) and double-charged cations is not enough to ensure a selective separation and then provide higher concentration factors.

The SEDF model allowed to determine the membrane permeances to ions (Na^+, SO_4^{2-} an H^+). When those values were compared with others from studies at neutral pH, they reflected the effects of chemical speciation and the changes of acid-base properties of the membrane. SEDF model based on Na_2SO_4 (dominant salt) was suitable to fit the experimental data and showed that feed pH and chemical composition are key parameters affecting rejection and trans-membrane flux.

NF270 membrane was able to concentrate the metal ions (up to a factor of 2), while HydraCoRe concentrated metals 1.5 times. NF270 also allowed to obtain a dilute sulfuric acid stream with some impurities (mainly Fe(II)) as permeate. This process will be more effective in solutions with higher sulfuric concentrations, which could lead to lower acid rejections. Moreover, HydraCoRe 70pHT membrane allowed to remove the acidity from the effluent. Although metals were concentrated, it was possible to obtain a richer stream of sulfuric acid, but with more impurities in solution.

Acknowledgments

This research was supported by the Waste2Product project (CTM2014-57302-R) financed by the Ministerio de Economía y Competitividad (MINECO) and the Catalan Government (Project Ref. 2014SGR50), Spain. The work of Julio López was supported by the Spanish Ministry (MINECO)

within the scope of the grant BES-2015-075051. We would like to acknowledge the contribution of M. Galindo to the project.

Nomenclature

c_s'	salt concentration in the feed solution (mol·m^{-3})
$c_s^{(m)}$	salt concentration in the solution adjacent to the membrane surface (mol·m^{-3})
c_s''	salt concentration in the permeate (mol·m^{-3})
c_t'	trace ion concentration in the feed solution (mol·m^{-3})
$c_t^{(m)}$	trace ion concentration in the solution adjacent to the membrane surface (mol·m^{-3})
c_t''	trace ion concentration in the permeate (mol·m^{-3})
D_i	ion diffusion coefficient in the membrane (m^2·s^{-1})
$D_i^{(\delta)}$	solute diffusion coefficient in the concentration-polarization layer (m^2·s^{-1})
$D_{\pm}^{(\delta)}$	dominant ion diffusion coefficients in the concentration-polarization layer (m^2·s^{-1})
$D_s^{(\delta)}$	dominant salt diffusion coefficient in the concentration-polarization layer (m^2·s^{-1})
$D_t^{(\delta)}$	trace ion diffusion coefficient in the concentration-polarization layer (m^2·s^{-1})
f_s	reciprocal dominant salt trans-membrane transfer
f_t	reciprocal trace ion trans-membrane transfer
J_v	trans-membrane flux (μm·s^{-1})
$P_s^{(\delta)}$	concentration-polarization layer permeance to the dominant salt (m·s^{-1})
P_s	membrane permeance to the dominant salt (m·s^{-1})
$P_{\pm}$	membrane permeances to the dominant ions (m·s^{-1})
P_t	membrane permeances to the trace ions (m·s^{-1})

Pe_s	dominant salt Péclet number
Pe_t	trace ion Péclet number
R_s^{int}	dominant salt intrinsic rejection
R_t^{int}	trace ion intrinsic rejection
R_s^{obs}	dominant salt observable rejection
R_t^{obs}	trace ion observable rejection
Z_i	ion charge
$Z_{\pm}$	dominant ion charges
Z_t	trace ion charge
Greek letters	
α	fraction of trace ion over salt diffusion coefficients in the concentration polarization-layer
δ	estimated concentration-polarization thickness (m)

498

499

Annex I – Speciation diagrams

Table A1.1. Chemical equilibrium constants at 25ºC for the reactions considered in this study

Chemical reaction	- logK
$Na^+ + SO_4^{2-} \leftrightarrow NaSO_4^-$	0.70
$H^+ + SO_4^{2-} \leftrightarrow HSO_4^-$	1.98
$Fe^{2+} + SO_4^{2-} \leftrightarrow FeSO_4$	2.25
$Fe^{2+} + H^+ + SO_4^{2-} \leftrightarrow FeHSO_4^+$	3.07
$Cu^{2+} + SO_4^{2-} \leftrightarrow CuSO_4$	2.31
$Zn^{2+} + SO_4^{2-} \leftrightarrow ZnSO_4$	2.37
$Zn^{2+} + 2\ SO_4^{2-} \leftrightarrow Zn(SO_4)_2^{2-}$	3.28

Table A1.2 collects the chemical speciaton diagrams for the two kinds of water tested: a) 0.1 M Na_2SO_4 and b) a solution mimicking AMD from dams, containing Na_2SO_4 and Fe, Zn and Cu.

Table A1.2. Chemical speciation diagrams for Na_2SO_4 solutions with and without metals (Cu, Zn, Fe)

	Na_2SO_4 solution	Na_2SO_4 solution with metallic ions (Cu,Zn,Fe)
H	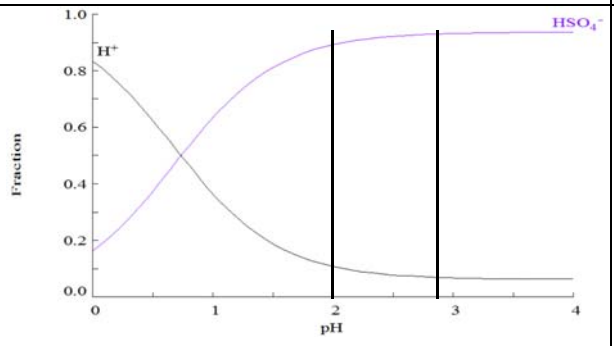	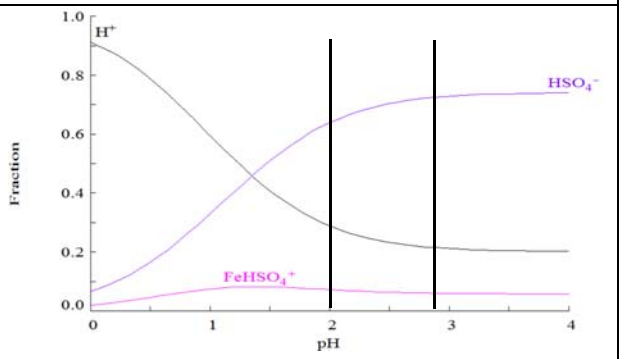

Na	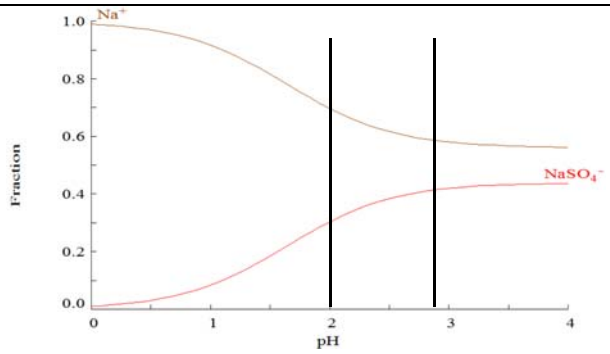 Na+ NaSO4- Fraction pH	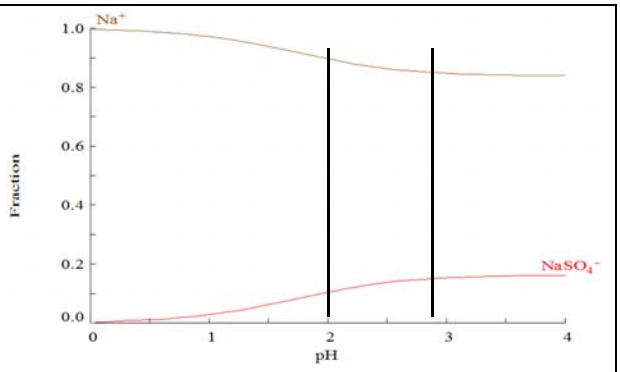 Na+ NaSO4- Fraction pH
SO_4	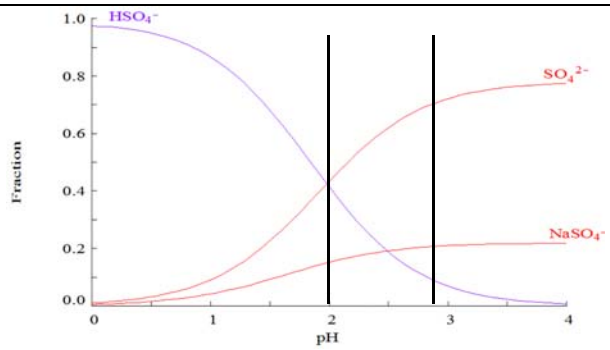 HSO4- SO4 2- NaSO4- Fraction pH	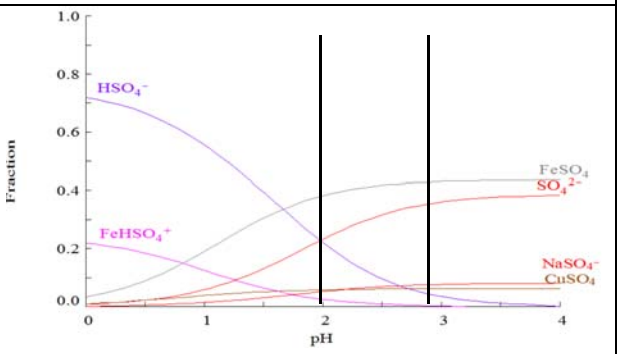 HSO4- FeSO4 SO4 2- FeHSO4+ NaSO4- CuSO4 Fraction pH
Fe		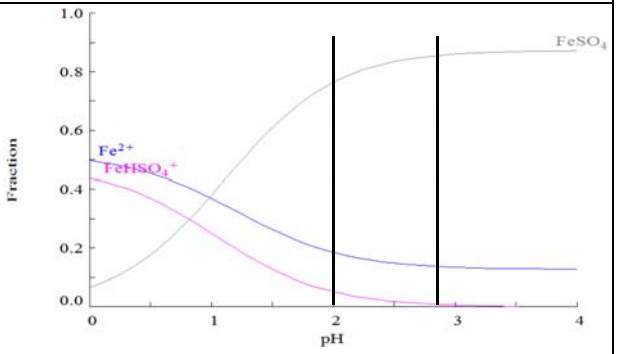 FeSO4 Fe2+ FeHSO4+ Fraction pH
Zn		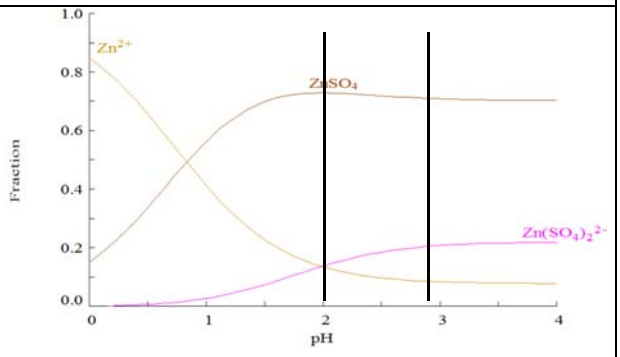 Zn2+ ZnSO4 Zn(SO4)2 2- Fraction pH

Cu		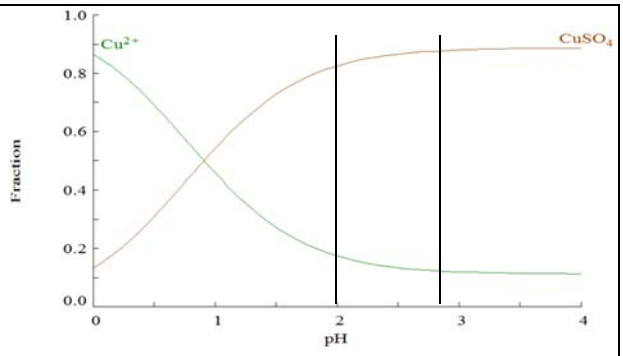

509

510 **References**

511

512 [1] E. Macingova, A. Luptakova, Recovery of metals from acid mine drainage, Chem. Eng.
513 Trans. 28 (2012) 109–114. doi:10.3303/CET1228019.

514 [2] A.S. Sheoran, V. Sheoran, Heavy metal removal mechanism of acid mine drainage in
515 wetlands: A critical review, Miner. Eng. 19 (2006) 105–116.
516 doi:10.1016/j.mineng.2005.08.006.

517 [3] D.B. Johnson, K.B. Hallberg, Acid mine drainage remediation options: A review, Sci. Total
518 Environ. 338 (2005) 3–14. doi:10.1016/j.scitotenv.2004.09.002.

519 [4] D.W. Blowes, C.J. Ptacek, J.L. Jambor, C.G. Weisener, D. Paktunc, W.D. Gould, D.B.
520 Johnson, The Geochemistry of Acid Mine Drainage, in: Treatise on Geochemistry,
521 Elsevier, 2014: pp. 131–190. doi:10.1016/B978-0-08-095975-7.00905-0.

522 [5] G.S. Simate, S. Ndlovu, Acid mine drainage: Challenges and opportunities, J. Environ.
523 Chem. Eng. 2 (2014) 1785–1803. doi:10.1016/j.jece.2014.07.021.

524 [6] D.B. Johnson, Chemical and Microbiological Characteristics of Mineral Spoils and
525 Drainage Waters at Abandoned Coal and Metal Mines, Water, Air Soil Pollut. Focus. 3
526 (2003) 47–66. doi:10.1023/A:1022107520836.

527 [7] A. Akcil, S. Koldas, Acid Mine Drainage (AMD): causes, treatment and case studies, J.
528 Clean. Prod. 14 (2006) 1139–1145. doi:10.1016/j.jclepro.2004.09.006.

[8] N. Kuyucak, Acid mine drainage prevention and control options, Mine, Water Environ. 95 (1999) 96–102.

[9] N.O. Egiebor, B. Oni, Acid rock drainage formation and treatment: a review, Asia-Pacific J. Chem. Eng. 2 (2007) 47–62. doi:10.1002/apj.57.

[10] O. Dianrdo, P.D. Kondos, D.J. Mackinnon, R.G.L. McGready, P.A. Riveros, M. Skaff, Study on metals recovery/recycling from acid mine drainage, MEND Treat. Comm. (1991). doi:10.1017/CBO9781107415324.004.

[11] M.A. Caraballo, F. Macías, T.S. Rötting, J.M. Nieto, C. Ayora, Long term remediation of highly polluted acid mine drainage: A sustainable approach to restore the environmental quality of the Odiel river basin, Environ. Pollut. 159 (2011) 3613–3619. doi:10.1016/j.envpol.2011.08.003.

[12] M. Kalin, A. Fyson, W.N. Wheeler, The chemistry of conventional and alternative treatment systems for the neutralization of acid mine drainage, Sci. Total Environ. 366 (2006) 395–408. doi:10.1016/j.scitotenv.2005.11.015.

[13] C. Costello, Acid Mine Drainage : Innovative Treatment Technologies Prepared by Technology Innovation Office, U.S. Environ. Prot. Agency, Off. Solid Waste Emerg. Response. (2003). https://clu-in.org/download/studentpapers/costello_amd.pdf.

[14] J. Fripp, P.F. Ziemkiewicz, H. Charkavorki, Acid Mine Drainage Treatment, in: EMRRP-SR-14, 2000. https://sav.el.erdc.dren.mil/elpubs/pdf/sr14.pdf (accessed June 8, 2017).

[15] PIRAMID Consortium, Engineering guidelines for the passive remediation of acidid and/or metalliferous mine drainage and similar wastewaters, 2003. doi:10.1016/j.ecoleng.2008.08.016.

[16] F. Fu, Q. Wang, Removal of heavy metal ions from wastewaters: A review, J. Environ. Manage. 92 (2011) 407–418. doi:10.1016/j.jenvman.2010.11.011.

[17] D. Howard, C. Gobler, G. Robinson, R, E, P.M. Cole, Sustainable purification of mine

554 water using ion exchange technology, Abstr. Int. Mine Water Conf. Pretoriam South
555 Africa. (2009) 447–453.
556 [18] H. Al-Zoubi, A. Rieger, P. Steinberger, W. Pelz, R. Haseneder, G. Härtel, Optimization
557 Study for Treatment of Acid Mine Drainage Using Membrane Technology, Sep. Sci.
558 Technol. 45 (2010) 2004–2016. doi:10.1080/01496395.2010.480963.
559 [19] H. Al-Zoubi, A. Rieger, P. Steinberger, W. Pelz, R. Haseneder, G. Härtel, Nanofiltration of
560 Acid Mine Drainage, Desalin. Water Treat. 21 (2010) 148–161.
561 doi:10.5004/dwt.2010.1316.
562 [20] X. Tongwen, Electrodialysis processes with bipolar membranes (EDBM) in environmental
563 protection—a review, Resour. Conserv. Recycl. 37 (2002) 1–22. doi:10.1016/S0921-
564 3449(02)00032-0.
565 [21] M.M.A. Shirazi, A. Kargari, M. Tabatabaei, A.F. Ismail, T. Matsuura, Assessment of
566 atomic force microscopy for characterization of PTFE membranes for membrane
567 distillation (MD) process, Desalin. Water Treat. 54 (2015) 295–304.
568 doi:10.1080/19443994.2014.883576.
569 [22] S. You, J. Lu, C.Y. Tang, X. Wang, Rejection of heavy metals in acidic wastewater by a
570 novel thin-film inorganic forward osmosis membrane, Chem. Eng. J. 320 (2017) 532–538.
571 doi:10.1016/j.cej.2017.03.064.
572 [23] B.C. Ricci, C.D. Ferreira, A.O. Aguiar, M.C.S. Amaral, Integration of nanofiltration and
573 reverse osmosis for metal separation and sulfuric acid recovery from gold mining effluent,
574 Sep. Purif. Technol. 154 (2015) 11–21. doi:10.1016/j.seppur.2015.08.040.
575 [24] M. Mullett, R. Fornarelli, D. Ralph, Nanofiltration of mine water: impact of feed pH and
576 membrane charge on resource recovery and water discharge, Membranes (Basel). 4
577 (2014) 163–180. doi:10.3390/membranes4020163.
578 [25] T.J.K. Visser, S.J. Modise, H.M. Krieg, K. Keizer, The removal of acid sulphate pollution

by nanofiltration, Desalination. 140 (2001) 79–86.

[26] K. Soldenhoff, J. Mcculloch, A. Manis, P. Macintosh, Nanofiltration in metal and acid recovery, in: Nanofiltration - Princ. Appl., 2005: pp. 460–478.

[27] I.W. Van der Merwe, Application of nanofiltration in metal recovery, J. South African Inst. Min. Metall. 98 (1998) 339–341.

[28] R. Cameron, C. Edwards, Membrane technology applications in mineral processing, Proc. 44th Annu. Can. Miner. Process. Oper. Conf. Ottawa, Ontario, Canada. (2012).

[29] M.P. González, R. Navarro, I. Saucedo, M. Avila, J. Revilla, C. Bouchard, Purification of phosphoric acid solutions by reverse osmosis and nanofiltration, Desalination. 147 (2002) 315–320. doi:10.1016/S0011-9164(02)00558-1.

[30] C.-M. Zhong, Z.-L. Xu, X.-H. Fang, L. Cheng, Treatment of Acid Mine Drainage (AMD) by Ultra-Low-Pressure Reverse Osmosis and Nanofiltration, Environ. Eng. Sci. 24 (2007) 1297–1306. doi:10.1089/ees.2006.0245.

[31] R. Fornarelli, M. Mullett, D. Ralph, Factors influencing nanofiltration of acid mine drainage, Reliab. Mine Water Technol. (2013) 563–568.

[32] A. Yaroshchuk, X. Martínez-Lladó, L. Llenas, M. Rovira, J. de Pablo, J. Flores, P. Rubio, Mechanisms of transfer of ionic solutes through composite polymer nano-filtration membranes in view of their high sulfate/chloride selectivities, Desalin. Water Treat. 6 (2009) 48–53.

[33] A. Yaroshchuk, M.L. Bruening, E.E. Licón Bernal, Solution-Diffusion-Electro-Migration model and its uses for analysis of nanofiltration, pressure-retarded osmosis and forward osmosis in multi-ionic solutions, J. Memb. Sci. 447 (2013) 463–476. doi:10.1016/j.memsci.2013.07.047.

[34] A. Yaroshchuk, X. Martínez-Lladó, L. Llenas, M. Rovira, J. de Pablo, Solution-diffusion-film model for the description of pressure-driven trans-membrane transfer of electrolyte

mixtures: One dominant salt and trace ions, J. Memb. Sci. 368 (2011) 192–201. doi:10.1016/j.memsci.2010.11.037.

[35] N. Pages, A. Yaroshchuk, O. Gibert, J.L. Cortina, Rejection of trace ionic solutes in nanofiltration : Influence of aqueous phase composition, Chem. Eng. Sci. 104 (2013) 1107–1115. doi:10.1016/j.ces.2013.09.042.

[36] A. Yaroshchuk, M.L. Bruening, An analytical solution of the solution-diffusion-electromigration equations reproduces trends in ion rejections during nanofiltration of mixed electrolytes, J. Memb. Sci. 523 (2017) 361–372. doi:10.1016/j.memsci.2016.09.046.

[37] Proyecto Rio Tinto, (n.d.). http://riotinto.atalayamining.com/la-mina/ (accessed June 22, 2017).

[38] I. Puigdomenech, Chemical equilibirum software Hydra/Medusa, (2001). https://sites.google.com/site/chemdiagr/home.

[39] A. Simon, W.E. Price, L.D. Nghiem, Impact of chemical cleaning on the nanofiltration of pharmaceutically active compounds (PhACs): The role of cleaning temperature, J. Taiwan Inst. Chem. Eng. 44 (2013) 713–723. doi:10.1016/j.jtice.2013.01.030.

[40] J.E. Tomaschke, A.J. Testa, J.G. Vouros, Stable membranes from sulfonated polyarylethers, US4990252 A, 1989.

[41] K. Ikeda, S. Yamamoto, H. Ito, Sulfonated polysulfone composite semipermeable membranes and process for producing the same, US4818387 A, 1989.

[42] K. Ikeda, T. Nakano, H. Ito, T. Kubota, S. Yamamoto, New composite charged reverse osmosis membrane, Desalination. 68 (1988) 109–119. doi:10.1016/0011-9164(88)80048-1.

[43] R.N. Franks, J. Van Bourg, S. McMorrow, C.R. Bartels, A nanofiltration membrane for the removal of color and disinfection byproducts from surface water to meet state and federal

629 standards, Proc. AMTA/AWWA Membr. Technol. Conf. Orlando, FL, 2015. (2015) 1–8.
630 [44] D. Breite, M. Went, A. Prager, A. Schulze, The critical zeta potential of polymer
631 membranes: how electrolytes impact membrane fouling, RSC Adv. 6 (2016) 98180–
632 98189. doi:10.1039/C6RA19239D.
633 [45] D.A. Sotto, Aplicación de la tecnología de membranas de nanofiltración y ósmosis inversa
634 para el tratamiento de disoluciones acuosas de compuestos fenólicos y ácidos
635 carboxílicos, Universidad Rey Juan Carlos, 2008.
636 [46] R. Chennamsetty, I. Escobar, Evolution of a Polysulfone Nanofiltration Membrane
637 following Ion Beam Irradiation, Langmuir. (2008) 5569–5579.
638 [47] N. Pagès, M. Reig, O. Gibert, J.L. Cortina, Trace ions rejection tunning in NF by selecting
639 solution composition: Ion permeances estimation, Chem. Eng. J. 308 (2017) 126–134.
640 doi:10.1016/j.cej.2016.09.037.
641 [48] G. Artuğ, I. Roosmasari, K. Richau, J. Hapke, A Comprehensive Characterization of
642 Commercial Nanofiltration Membranes, Sep. Sci. Technol. 42 (2007) 2947–2986.
643 doi:10.1080/01496390701560082.
644 [49] A.E. Yaroshchuk, Dielectric exclusion of ions from membranes, Adv. Colloid Interface Sci.
645 85 (2000) 193–230. doi:10.1016/S0001-8686(99)00021-4.
646 [50] Y. Tanaka, Ion exchange membranes : fundamentals and applications, 2nd ed., 2015.
647 https://books.google.es/books?id=au1DBAAAQBAJ&pg=PA156&lpg=PA156&dq=pK+in+i
648 on+exchange+membranes&source=bl&ots=ofnJP3i4Sp&sig=T4sNFqItnHZSsWsuHSril26
649 wx64&hl=es&sa=X&ved=0ahUKEwjE36G40snUAhUBvxQKHWojCgIQ6AEITjAG#v=onep
650 age&q&f=false.
651 [51] B.A.M. Al-Rashdi, D.J. Johnson, N. Hilal, Removal of heavy metal ions by nanofiltration,
652 Desalination. 315 (2013) 2–17. doi:10.1016/j.desal.2012.05.022.
653 [52] I. Dammak, M.A. Neves, H. Nabetani, H. Isoda, S. Sayadi, M. Nakajima, Transport

654 properties of oleuropein through nanofiltration membranes, Food Bioprod. Process. 94
655 (2015) 342–353. doi:10.1016/j.fbp.2014.04.002.
656 [53] M. Reig, N. Pagès, E. Licon, C. Valderrama, O. Gibert, A. Yaroshchuk, J.L. Cortina,
657 Evolution of electrolyte mixtures rejection behaviour using nanofiltration membranes under
658 spiral wound and flat-sheet configurations, Desalin. Water Treat. 56 (2015) 3519–3529.
659 doi:10.1080/19443994.2014.974215.
660